

PAPER • OPEN ACCESS

Investigation of design space in manufacturing meta-biomaterials by additive manufacturing

To cite this article: Siti Rohaida Mohamed and Saiful Anwar Che Ghani 2021 *IOP Conf. Ser.: Mater. Sci. Eng.* **1078** 012024

View the [article online](#) for updates and enhancements.

You may also like

- [Effective elastic properties of doubly periodic array of functionally graded inclusions by an iterative FE-BE coupling method](#)
Z Y Liu, D Li, Y C Xie et al.
- [Design of lead-free PVDF/CNT/BaTiO₃ piezocomposites for sensing and energy harvesting: the role of polycrystallinity, nanoadditives, and anisotropy](#)
Jagdish A Krishnaswamy, Federico C Buroni, Enrique Garcia-Macias et al.
- [Metasurfaces: a new look at Maxwell's equations and new ways to control light](#)
M A Remnev and V V Klimov



The Electrochemical Society
Advancing solid state & electrochemical science & technology

241st ECS Meeting

May 29 – June 2, 2022 Vancouver • BC • Canada

Extended abstract submission deadline: Dec 17, 2021

Connect. Engage. Champion. Empower. Accelerate.
Move science forward



Submit your abstract



Investigation of design space in manufacturing meta-biomaterials by additive manufacturing

Siti Rohaida Mohamed^{1,*} and Saiful Anwar Che Ghani¹

¹Faculty of Mechanical and Automotive Engineering Technology, Universiti Malaysia Pahang, 26600, Pekan, Pahang, Malaysia.

*Corresponding author's e-mail: sitiroida0603@gmail.com

Abstract. Topology features such as interconnectivity, pore shape and size, porosity, struts thickness, and used materials play the key roles for mechanical and biological properties of meta-biomaterials structures. However, the influences of morphological geometries on the mechanical and biological properties are not certainly intuitive. This paper develops parametric model that use to visualize the morphological geometries of unit cell of meta-biomaterials on design space that governing the manufacturing limitation, mechanical and biological requirements. The selected samples within design spaces tested to determine manufacturing accuracy and effective elastic modulus by finite element analysis. The geometries discrepancies between designed models and manufactured samples obtained percentage of average errors of 13% for diamonds structures and 21% for square structures. The proposed technique yielded average error reduced to 74.4% for diamond structures and 44.4% for square structures of effective elastic modulus from theoretical calculation. The approach and the implications of the results discussed in the context of mechanical and biological criteria with highlight of advantages and limitations of meta-biomaterials manufactured by additive manufacturing for orthopaedic implants.

Keywords: Meta-biomaterials; Additive Manufacturing; Finite Element Analysis; CoCrMo.

1. Introduction

Meta-biomaterials known as a unique class of materials that exhibited unprecedented combination of mechanical, mass transport and biological properties made from biomaterials for biomedical applications [1, 2]. Metamaterials are design with a repeating unit cell and used for other applications including optical [3, 4] and acoustic [5, 6] given to micro-architecture level. Bone-mimicking meta-biomaterials are progressively being studied which are particularly relevant for bone substitution since the implants offer a high surface area to promote bone in-growth, facilitate transportation of nutrient components, expedite tissue regeneration as well as improve implant longevity [7]. In addition, the mechanical properties of meta-biomaterials ideally tailored to have comparable elastic modulus with human bone as to reduce stress-shielding phenomenon that influence bone resorptions and revision surgeries.

The reliability to manufacture meta-biomaterials with highly controlled micro geometry architectures is vital to the great achievement of orthopaedic implants. Conventional techniques for example, space holder [8, 9] and direct metal foaming [10, 11] provide restricted freedom in fabricating complex structures with desired porosity and homogenous pore distribution and



interconnectivity that can fulfill specific requirements of mechanical properties and biological response [12-14]. Recently, additive manufacturing (AM) technology such as electron beam melting (EBM) and selective laser melting (SLM), bring versatility in three-dimensional (3D) layer-by-layer processes of patient-specific implant devices [15-17]. Additionally, gradient of pore size and porosity are introduced into the micro-architecture to improve mechanical behaviour and biological response with the respect of anatomical location of local bone.

The micro-architectures of the unit cell of meta-biomaterials customized with rationally controlled pore shape, pore size, and porosity to provide sufficient mechanical stability and optimum structural suitability for bone-implant interactions [18, 19]. From previous studies, topological design of unit cell meta-biomaterials, relative density and used materials influenced the compressive and fatigue properties of the structures [20-22]. For meta-biomaterials, there are presently no quantitative standards of specifying pore parameters and porosity volume constraints for cells in-growth and mechanical stability of the implants. Furthermore, there is lack of study that discussed the effects of unit cell size, porosity percentage, and strut thickness on the mechanical and biological properties of meta-biomaterials particularly for orthopaedic implant applications.

Many recent studies are focusing on selection of unit cell topologies of porous biomaterials with no systematic approach to obtain designed structures that are manufacturable for implants [23, 24]. However, this method does not provide a full perspective of the precise viable design space to define each unit cell topological parameters. Additionally, this technique frequently leads to design and produce porous implants with geometrical parameters higher than the ideal range for biological properties requirements. Any insight into how the topologies design, biological and manufacturing requirements influenced the acceptable parameter design range of a unit cell of meta-biomaterials. In essence, an extensive characterization of the developed design space for meta-biomaterials is crucial to comprehend the relationship of mechanical properties and biological requirements with the geometrical design boundaries.

This paper presents systematic procedure for understanding the interaction relationship between geometrical parameters with the mechanical and biological properties. The chart model allows graphically examining the acceptable porosity percentage, unit cell size, strut thickness and pore size that are possible for fabricating process. This work also goals to investigate the purpose of design space in manufacturing meta-biomaterials by SLM, as well as to comprehend the relationship of with geometrical constraints inflicted by biological necessities, mechanical requirements and additive manufacturing drawback.

2. Methodology

2.1. Development of cell topologies design domains

The parametric geometrical of diamond and square unit cell types were applied to develop the design domains. Both unit cells have modulus matrix with cubic symmetry. The designed unit cells exhibited almost isotropic mechanical properties. From the given geometric topology, computer-aided design (CAD) models generated via SolidWorks software. The overall unit cell type controlled by two parameters, which were strut thickness (t) and unit cell size (l). These parameters combination regulated each unit cell to obtain resultant of desired porosity and pore size. In this study, the pore size defined by the largest circle correspond that can permit through adjacent cells in the samples. The porosity derived as in equation 1.

$$Porosity (\%) = \left(1 - \frac{v_p}{v_s}\right) \times 100 \quad (1)$$

where v_p refers to void volume of unit cell and v_s refers to the volume of solid unit cell. The pore sizes and porosities plotted in contour design spaces where on the x -axis represented pore size and the y -axis represented strut thickness. Meanwhile, isometric lines illustrated the value of cell size and porosity of the structures. From contour area, the accompanying biomechanical requirements and fabrication

limits overlaid to feature the allowable design maps as in figure 1 and figure 2. The according vital criteria for generating design space as follows:

- Biological requirement: Pore size range of 50 μm and 800 μm with porosity more than 50% are favourable for optimum biological response. The red lines showed the boundaries of these values in the design space maps.
- Manufacturing constraint: Additive manufacturing (AM) technologies restricted to manufacture a minimal strut thickness of 300 μm of meta-biomaterials depending to selected process parameters. The constraint illustrated in the *x-axis* design space maps as in red line.

The design domain maps develops with borders as in the blue region represents the geometric parameters with respect to appropriate for bone in-growth and manufacture capability of AM technology. All the designs of meta-biomaterials falling within the domains area were satisfactory solutions that emerge the bone in-growth requirements and AM limitations.

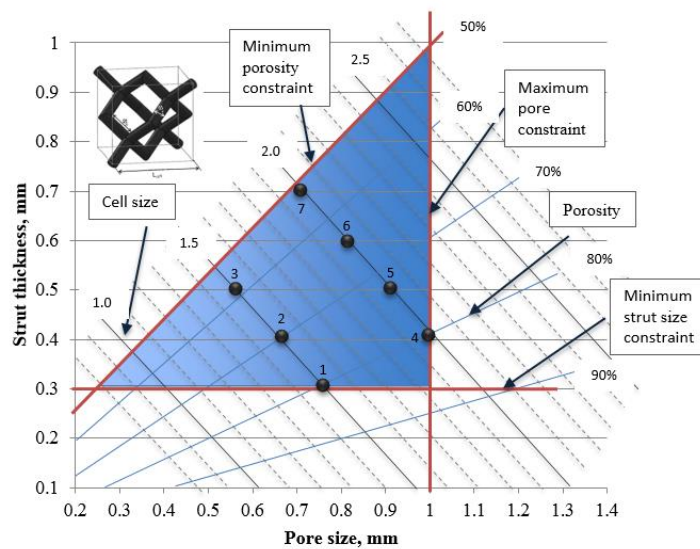


Figure 1. Admissible design space for diamond type.

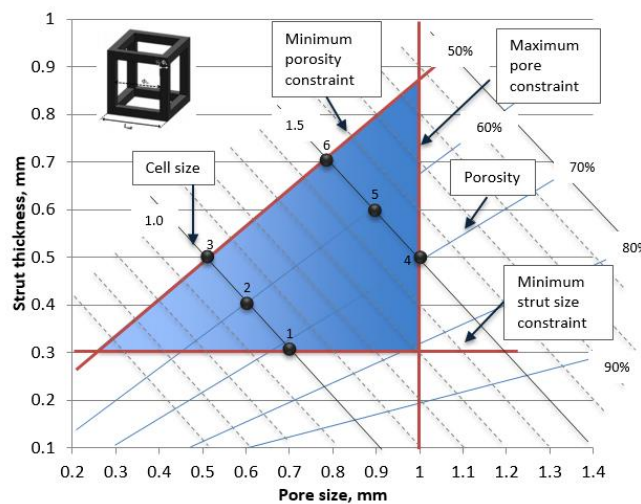


Figure 2. Admissible design space for square type.

2.2. Design parameters of selected samples

The representative samples (in black) at the boundary of the design spaces as in figure 1 and figure 2 selected for further investigation. Seven points of diamond type designated with the porosity in the range of 50% to 80% (Diamond #1-7). Meanwhile, for square unit cell, six points were selected in the range of porosity of 50% to 70% (Square #1-6). These points considered direct correlation of the consequence of geometrical parameters with morphology corresponding to ideal requirement of orthopaedic implants. Table 1 summarises the morphological details for the selected points.

Table 1. Geometrical details of the representative samples.

Unit cell type	#	Unit cell size (mm)	Strut thickness (mm)	Pore size (mm)	Porosity (%)
Diamond	1	1.5	0.3	0.76	82
	2	1.5	0.4	0.66	70
	3	1.5	0.5	0.56	58
	4	2.0	0.4	1.1	80
	5	2.0	0.5	0.91	74
	6	2.0	0.6	0.81	66
	7	2.0	0.7	0.71	54
Square	1	1.0	0.3	0.70	70
	2	1.0	0.4	0.60	60
	3	1.0	0.5	0.50	50
	4	1.5	0.5	1.0	70
	5	1.5	0.6	0.9	60
	6	1.5	0.7	0.80	50

2.3. Material and fabrication process

The selected geometries fabricated by SLM process (SLM® 125HL) out of cobalt chrome molybdenum (CoCrMo) alloys with powder particles had average size of approximately 22 μm . The manufacturing process used 300 W laser and laser spot diameter of 80 μm with energy density 119 J/mm^3 . The samples manufactured at intervals of 30 μm layer thicknesses and hatch spacing of 120 μm with layer-by-layer exposure on a stainless steel base plate. The build chamber was flushed with argon gas to prevent contamination and oxidation. The samples experienced thermal stress-relieved at temperature of 1050 $^{\circ}\text{C}$ for two (2) hours in an argon atmosphere. Electrical discharge machining (EDM) used to detach the build samples from the base plate.

2.4. Morphology evaluations

Each design points were randomly selected and morphological evaluated in order to measure as manufactured strut thickness and pore size. The strut size of produced samples investigated and analyzed in addressing the manufacturability and accuracy of SLM performance of the produced meta-biomaterials using optical microscope (Dino-lite Digital Microscope). These average values measured as ten dimensional values at random points for every measurement. The results were compared to the as CAD designed strut thickness and pore size.

2.5. Prediction of effective elastic modulus

A model proposed by Gibson and Ashby [25] was employed in order to predict the effective elastic modulus of designed samples as in equation 2. Elastic modulus of solid Co-Cr-Mo was consumed as 220 GPa [26].

$$E^*/E_s = C(\rho^*/\rho_s)^2 \quad (2)$$

where E^* = Elastic modulus of meta-biomaterials;

E_s = Elastic modulus of solid;

C = Constant;

ρ^* = Density of meta-biomaterials; and

ρ_s = Density of solid

From above equation, elastic modulus demonstrated that was dependent on the relevant density. Equation 3 used to determine the relevant density that associated to porosity volume [25].

$$(\rho^*/\rho_s) = 1 - \varphi \quad (3)$$

where φ was the porosity. Then, equation 3 rewritten as equation 4 in order to determine the effective elastic modulus [25].

$$E_{eff} = E_s (1 - \varphi)^2 \quad (4)$$

where E_{eff} = effective elastic modulus

Gibson and Ashby model was employed in this study for prediction effective elastic modulus (E_{eff}) of three-dimensional porous structure when the structure loaded vertically upon unit cell geometry. ANSYS 18.0 also used to predict the effective elastic modulus of the samples. In order to explore what impact this has on the effective stiffness, the study considered the effect of variable within unit cell parameters. Finite element model was designed with a structure that having six layers with one unit cell in each layer. SOLID 185 used to mesh each model by four node tetrahedral elements with size of element of 0.1 mm. Under the materials elastic limit, a uniform 0.1% compressive strain applied to the top surface of the model, while fixed at the bottom. No boundary constraints added to the sides of the model. Due to its impact on simulation accuracy and computational time, the influence of mesh configuration was a vital consideration in structural analysis [27, 28]. Results of effective elastic modulus obtained from mesh sensitivity compared with theoretical CoCrMo materials properties as 200 GPa. The mesh element size from 0.05 mm to 0.5 mm and quadrilateral element used to study the mesh independent.

3. Results and discussion

3.1. Physical manufacturability

Table 2 summaries the measurement and averages of errors of struts thickness and pore size of produced meta-biomaterials. From the table, the averages strut thickness error for diamonds structures is 13% and 21% for square structures. Meanwhile, average error of the pore sizes for diamond structures is 1.8% and 1.4% for square structures. The struts thickness and pore sizes measured for the diamond structures are in good agreement with the as-designed strut sizes for sample D#3, D#5 - D#7. Interestingly, the good manufacturing agreement with the self-supporting feature demonstrated in diamond structures due to angle of inclination between the two neighbouring strut layers. The inclination angle of strut has the potential to support the output of next layer after the previous scanned layer during the manufacturing activity [29, 30]. However, smaller strut sizes resulted in inaccuracy and shrinkage owed to loss connectivity among neighboring layers of unit cell. Hence, the strut size of diamond types with 0.3 and 0.4 mm are too thin for fabrication process. Furthermore, the strut angle

for diamond is lower than 45° from the horizontal plane or overhanging angle. Thus, deformation occurred during manufacturing process where the struts build on loose powder led to the defect on products [31, 32].

Meanwhile, the strut thickness of square type was higher than designed strut related to the initial measurement for the models. It caused the pore sizes results smaller than compared to as designed models for square structures. The increased of the strut thickness was the outcome of the partially melted powder particles added the strut core and melt pool size on the strut boundary. The average actual strut sizes were higher and pore sizes were smaller than CAD models. The overhang phenomenon occurred in the unsupported region on square unit cells as stresses led to dross formation and the partially melted powder particles added the average values of product's strut sizes. The short interaction of powder bed and heat source triggered by the scanning speed of laser beam led to rapid heating during the manufacturing process [34, 35]. Then, the melting phase followed significantly. The shrinkage in the components triggered this phenomenon. The results indicate that manufacturing errors were more susceptible to the strut thickness close to the manufacturing limits at high porosity volume.

Table 2. Manufacturability of meta-biomaterials.

Sample	Strut thickness (mm)	As-manufactured strut thickness (mm)	Error (%)	Pore size (mm)	As-manufactured pore size (mm)	Error (%)
D#1	0.3	0.29 ± 0.006	3.3	0.76	0.75 ± 0.006	1.32
D#2	0.4	0.39 ± 0.003	2.5	0.66	0.65 ± 0.003	1.52
D#3	0.5	0.50 ± 0	0	0.56	0.56 ± 0	0
D#4	0.4	0.29 ± 0.006	3.3	1.1	0.99 ± 0.005	10
D#5	0.5	0.50 ± 0	0	0.91	0.91 ± 0	0
D#6	0.6	0.60 ± 0	0	0.81	0.81 ± 0	0
D#7	0.7	0.70 ± 0	0	0.71	0.71 ± 0	0
S#1	0.3	0.31 ± 0.006	3.3	0.70	0.69 ± 0.006	1.42
S#2	0.4	0.41 ± 0.003	2.5	0.60	0.59 ± 0.006	1.67
S#3	0.5	0.51 ± 0.006	2	0.50	0.49 ± 0.003	2
S#4	0.5	0.51 ± 0.006	2	1.0	0.99 ± 0.006	1
S#5	0.6	0.61 ± 0.001	1.6	0.9	0.89 ± 0.006	1.11
S#6	0.7	0.71 ± 0.006	1.4	0.80	0.79 ± 0.01	1.25

3.2. FEA of effective elastic modulus

Originally, the developed Gibson and Ashby model used to predict the rigidity of the three-dimensional (3D) open cell structure when applied a load to unit cell structures that related approach used in this study [25]. Previous studies demonstrating the used of the Gibson and Ashby models were in harmony with the values obtained from mechanical testing [35, 36]. The effective elastic modulus derived from the mathematical calculation for each designed meta-biomaterials.

As the results, the effective elastic modulus of diamond type was ranging from 6.5 GPa to 42 GPa, and range of 18 GPa to 50 GPa for square type. Interestingly, the elastic modulus for higher volume porosity were met a good agreement as the values closer to the human bone properties (1-30 GPa). While further study mechanical properties through experimental was required, meta-biomaterials possessed load-bearing potential that allowed the structures to withstand severe cyclic loading

condition. In addition, geometrical design of meta-biomaterials inside the design domain had capacity for tailored porosity to imitate the mechanical properties of the host bone properties.

Mesh element size from 0.1 mm to 0.5 mm resulted effective elastic modulus of 169.23 GPa with accuracy 15.39% error. Mesh independent treatment was introduced to eliminate the geometric discretization error in complex morphologies of structures [37]. From finite element analysis, the effective modulus of diamond type ranging from 3.01 GPa to 4.79 GPa. Meanwhile, the effective modulus of square type ranging from 6.34 GPa to 28.75 GPa. Both diamond and square samples in the range of cancellous bone properties (1-15 GPa). Samples of square type of S#3, S#5 and S#6 exhibited elastic modulus similar to cortical bone properties (15-30 GPa) except for sample S#1 and S#4 which were in the range of cancellous bone. The results showed the pore structure could tailor the elastic modulus from the porosity value and different pore shape to produce accurate prediction of mechanical compressive behavior. Figure 3 illustrates the comparison of effective elastic modulus from Gibson and Ashby model and finite element analysis. The proposed technique yields accurate predictions for effective elastic modulus with decreasing of average error to 74.4% for diamond structures and 44.4% for square structures from theoretical calculation of Gibson and Ashby equation.

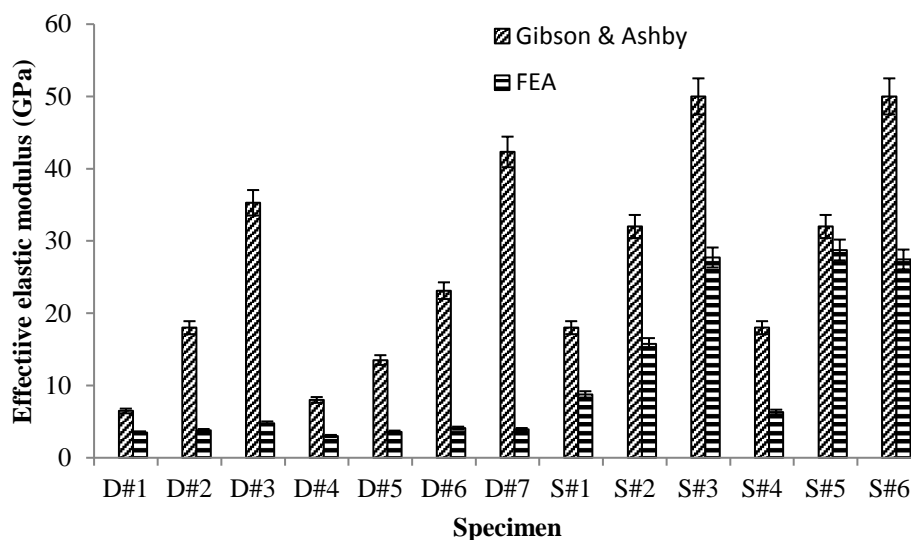


Figure 3. Effective elastic modulus of meta-biomaterials.

The FEA model showed substantially homogeneous deformation, beginning with buckling for both types and followed by complete compaction due to interaction between adjacent struts core. Figure 4 shows the deformation behaviours of the selected design structures predicted by FEA. It worth to note that FEA model was built for a fundamental analysis of deformation in porous structures. Particularly, this analysis emphasized the default options available for structural module in ANSYS software. In addition, the designed model based on controlled topologies where the strut surfaces can be irregular. This initiated flaws in manufacturing the structures as stress concentrators or added material to the struts by disputing compressive load. In addition, the mechanical properties of the meta-biomaterials might influenced by porosity and surface roughness, but those factors were not taken into account in the finite element analysis.

Both type of structures with different volume fractions deformed with same failure mechanism. Deformation mechanism represented plasticity for square and diamond type structures with 10%. From observation, the deformation commenced from the top and then, the structure collapsed by each layer of the cell continuously. The homogeneity of failure mechanism indicated the potential of high impact resistance from the struts of the samples [38]. Buckling micro-struts predicted to result in high-

energy releasing at respectively failure stage since the struts able to endure axial distortion due to their equivalent direction of load [39].

Failure of diamond type structures followed by shearing of the microscale struts led the structure to collapse as bending dominated deformation. Crushing struts to the center of plates contributed to a continuing shear fracture in 45° . Thus, in contrast with the buckling deformation of square structures, less energy released during collapse of diamond structure owing to its strut inclination angle. The findings indicated that orientation of strut play a key role in the mechanism of deformation and stress-strain compartments of the meta-biomaterials [39].

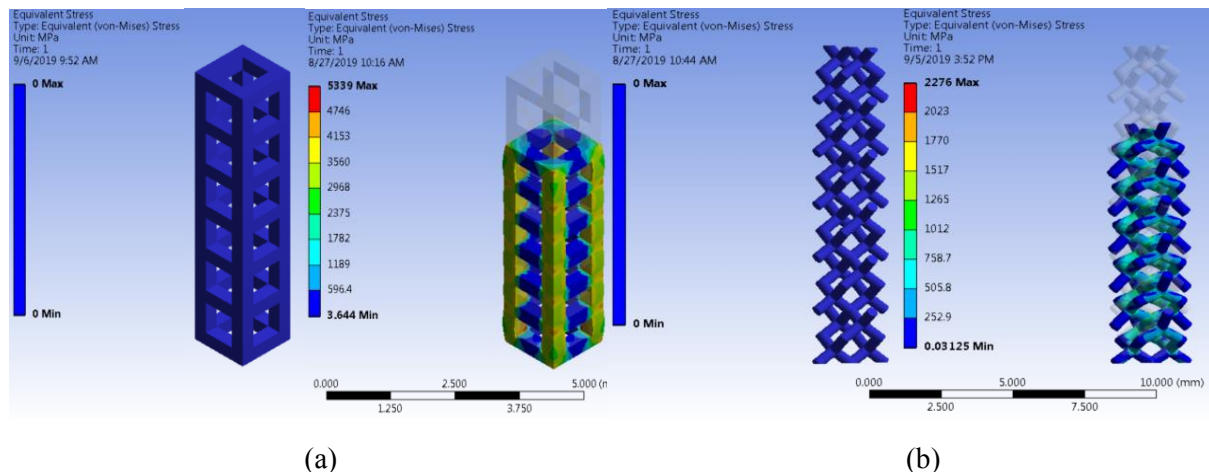


Figure 4. Deformation mechanism of (a) square and (b) diamond structures.

4. Conclusion

This paper presents two distinct meta-biomaterials topologies that are dependable for orthopaedic implants. This paper also successfully presented a technique for visually understanding the function of porosity and pore size as design variables of meta-biomaterials. In addition, the design space model showed how biological and mechanical requirements and manufacturing limitation can clearly incorporated in design topologies constraints that allow a holistic knowledge of the relationship of unit cell geometries on mechanical and biological requirements and manufacturing drawback. This method can help to clarify the factors that can influence the effectiveness of meta-biomaterials as orthopedic implants.

Morphological investigation had shown geometries deviations between CAD models and manufactured meta-biomaterials. The averages error of the strut thickness is 13% for diamonds structures and 21% for square structures. Meanwhile, average error of the pore sizes is 1.8% for diamond structures and 1.4% for square structures. The discrepancies predominantly attributed to the overhang phenomenon and partially melted powder particles. Manufacturing intolerance leads to reduction of pore size and shrinkage of the components. The prediction of elastic modulus confirmed that samples at higher porosity exhibit stiffness comparable to human bone with mean error decreased to 74.4% for diamond structures and 44.4% for square structures from theoretical calculation.

Acknowledgments

The authors gratefully acknowledge the financial support supported by the Malaysian Ministry of Higher Education and Universiti Malaysia Pahang (www.ump.edu.my) for Postgraduate Research Grants Scheme (PGRS1903164) and RDU200301.

References

- [1] Kolken H M, Janbaz S, Leeftang S M, Lietaert K, Weinans H H, Zadpoor A A 2018 *Materials Horizons* **5** 28-35.
- [2] Kolken H M A, Lietaert K, van der Sloten T, Pouran B, Meynen A, Van Loock G, et al. 2020 *Journal of the Mechanical Behavior of Biomedical Materials* **104** 103658.
- [3] Mahmud S, Islam S S, Mat K, Chowdhury M E H, Rmili H, Islam M T 2020 *Results in Physics* **18** 103259.
- [4] Forouzeshefard M R, Ghafari S, Vafapour Z 2021 *Journal of Luminescence* **230** 117734.
- [5] Ma K, Tan T, Yan Z, Liu F, Liao W-H, Zhang W 2020 *Nano Energy* 105693.
- [6] Ji G, Fang Y, Zhou J 2020 *Extreme Mechanics Letters* **36** 100648.
- [7] Ahmadi S M, Hedayati R, Li Y, Lietaert K, Tümer N, Fatemi A, et al. 2018 *Acta Biomaterialia* **65** 292-304.
- [8] Rodriguez-Contreras A, Punset M, Calero J A, Gil F J, Ruperez E, Manero J M 2021 *Journal of Materials Science & Technology* **76** 129-49.
- [9] Lu X Z, Lai C P, Chan L C 2020 *Materials & Design* **188** 108474.
- [10] Kim J, Hong D, Badshah M A, Lu X, Kim Y K, Kim S-m 2018 *Micromachines* **9** 376.
- [11] Ahmed N 2019 *Journal of Manufacturing Processes* **42** 167-91.
- [12] Pereira R F, Bártolo P J. 10.10 - Recent Advances in Additive Biomanufacturing. In: Yilbas S H F B J V T, editor. *Comprehensive Materials Processing*. Oxford: Elsevier; 2014. p. 265-84.
- [13] Javaid M, Haleem A 2018 *Journal of Clinical Orthopaedics and Trauma* **9** 202-6.
- [14] Kim T, See C W, Li X, Zhu D 2020 *Engineered Regeneration* **1** 6-18.
- [15] Li N, Huang S, Zhang G, Qin R, Liu W, Xiong H, et al. 2018 *Journal of Materials Science & Technology*.
- [16] Mitchell A, Lafont U, Hołyńska M, Semprimoschnig C 2018 *Additive Manufacturing* **24** 606-26.
- [17] Bartolomeu F, Costa M M, Alves N, Miranda G, Silva F S 2020 *Optics and Lasers in Engineering* **134** 106208.
- [18] Sobral J M, Caridade S G, Sousa R A, Mano J F, Reis R L 2011 *Acta Biomaterialia* **7** 1009-18.
- [19] Rahimizadeh A, Nourmohammadi Z, Arabnejad S, Tanzer M, Pasini D 2018 *Journal of the Mechanical Behavior of Biomedical Materials* **78** 465-79.
- [20] Che Ghani S A, Mohamed S R, Sha'ban M, Wan Harun W S, Md Noar N A Z 2020 *Procedia CIRP* **89** 79-91.
- [21] Xue R, Cui X, Zhang P, Liu K, Li Y, Wu W, et al. 2020 *Extreme Mechanics Letters* **40** 100918.
- [22] Mohamed S, Ghani S 2018 *Proceedings of Asia International Conference on Tribology 2018*: Malaysian Tribology Society.
- [23] Moussa A, Rahman S, Xu M, Tanzer M, Pasini D 2020 *Journal of the Mechanical Behavior of Biomedical Materials* **105** 103705.
- [24] Liu Y J, Ren D C, Li S J, Wang H, Zhang L C, Sercombe T B 2020 *Additive Manufacturing* **32** 101060.
- [25] Gibson L J, Ashby M F 1999 *Cellular solids: structure and properties* Cambridge university press).
- [26] Nakano T. 3 - Mechanical properties of metallic biomaterials. In: Niinomi M, editor. *Metals for Biomedical Devices*: Woodhead Publishing; 2010. p. 71-98.
- [27] Lim H, Battaile C C, Bishop J E, Foulk J W 2019 *International Journal of Plasticity* **121** 101-15
- [28] Huang X, Xie Y M 2007 *Finite Elements in Analysis and Design* **43** 1039-49.
- [29] Yan C, Hao L, Hussein A, Young P, Huang J, Zhu W 2015 *Materials Science and Engineering: A* **628** 238-46.
- [30] Pérez-Sánchez A, Yáñez A, Cuadrado A, Martel O, Nuño N 2018 *Materials & Design* **155** 106-15.
- [31] Harges C, Pöhl F, Röttger A, Thiele M, Theisen W, Esen C 2019 *Additive Manufacturing* **29** 100786.

- [32] Zhuang J, Gu D, Xi L, Lin K, Fang Y, Wang R 2020 *Powder Technology* **368** 59-69.
- [33] Wang P, Lei H, Zhu X, Chen H, Fang D 2019 *Journal of Alloys and Compounds* **789** 852-9.
- [34] Panda B K, Sahoo S 2019 *Results in Physics* **12** 1372-81.
- [35] Martin A A, Calta N P, Khairallah S A, Wang J, Depond P J, Fong A Y, et al. 2019 *Nature communications* **10** 1-10.
- [36] Jagodzinski D J, Miksch M, Aumann Q, Müller G 2020 *Mechanics Based Design of Structures and Machines* 1-15.
- [37] Zhu H, Lin Z, Peng J, Zhang H-Q, Zhu J, Zhang J 2020 *Heat Transfer Summer Conference and the ASME 2020 18th International Conference on Nanochannels, Microchannels, and Minichannels*: American Society of Mechanical Engineers Digital Collection.
- [38] Rashed M, Ashraf M, Mines R, Hazell P J 2016 *Materials & Design* **95** 518-33.
- [39] Kadkhodapour J, Montazerian H, Darabi A C, Anaraki A P, Ahmadi S M, Zadpoor A A, et al. 2015 *Journal of the Mechanical Behavior of Biomedical Materials* **50** 180-91.